

Propagation failure in excitable media

A. Hagberg*

Center for Nonlinear Studies and T-7, Theoretical Division, Los Alamos National Laboratory, Los Alamos, New Mexico 87545

E. Meron†

The Jacob Blaustein Institute for Desert Research and the Physics Department, Ben-Gurion University, Sede Boker Campus 84990, Sede Boker, Israel

(Received 15 July 1997)

We study a mechanism of pulse propagation failure in excitable media where stable traveling pulse solutions appear via a subcritical pitchfork bifurcation. The bifurcation plays a key role in that mechanism. Small perturbations, externally applied or from internal instabilities, may cause pulse propagation failure (wave breakup) provided the system is close enough to the bifurcation point. We derive relations showing how the pitchfork bifurcation is unfolded by weak curvature or advective field perturbations and use them to demonstrate wave breakup. We suggest that the recent observations of wave breakup in the Belousov-Zhabotinsky reaction induced by either an electric field [J.J. Taboada *et al.*, *Chaos* **4**, 519 (1994)] or a transverse instability [M. Markus, G. Kloss, and I. Kusch, *Nature (London)* **371**, 402 (1994)] are manifestations of this mechanism. [S1063-651X(97)11512-4]

PACS number(s): 05.45.+b, 82.20.Mj

I. INTRODUCTION

Failure of wave propagation in excitable media very often leads to the onset of spatiotemporal disorder. In the context of electrophysiology it may lead to ventricular fibrillation. Numerous studies have appeared in the past few years demonstrating conditions and mechanisms for failure of propagation in excitable and bistable media [3–9]. Failure may occur by external perturbations or spontaneously by intrinsic instabilities. Experimental examples include wave breakups in the excitable Belousov-Zhabotinsky (BZ) reaction induced by an electric field [1] and by a transverse instability [2].

Recently we have attributed domain breakup phenomena in bistable media to the proximity to a pitchfork front bifurcation illustrated schematically in Fig. 1(a) [10,11]. As shown in Fig. 1(b), near the bifurcation small perturbations, such as an advective field or curvature, unfold the pitchfork bifurcation to an S-shaped relation. If the perturbation is large enough to drive the system past the end point of a given front solution branch the front reverses direction. A local reversal event along an extended front line in a two-dimensional system involves the nucleation of a pair of spiral waves and is usually followed by domain breakup. The front bifurcation illustrated in Fig. 1(a) has been referred to in the literature as a nonequilibrium-Ising-Bloch (NIB) bifurcation [12,13].

In this paper we extend these ideas to wave breakups in excitable media. The NIB bifurcation is replaced in this case by a subcritical pitchfork pulse bifurcation as shown in Fig. 2(a). The typical unfolding of that bifurcation is shown in Fig. 2(b). Similar to the case of front solutions in bistable systems, perturbations that drive the system beyond the edge point of a given pulse branch may either reverse the direction

of pulse propagation or lead to pulse collapse and convergence to the stable uniform quiescent state [not shown in Fig. 2(b)]. The convergence to a uniform attractor is more likely to occur for pulse structures than for fronts and has always been observed in our simulations. Thus, in our study, the

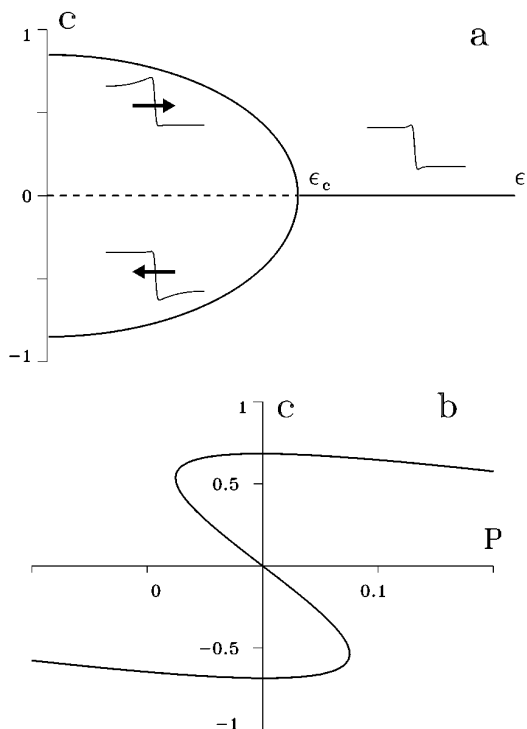


FIG. 1. Bifurcation diagrams for fronts in the bistable FHN reaction-diffusion system. (a) At the Nonequilibrium Ising-Bloch bifurcation a stationary front becomes unstable to a pair of counter-propagating fronts as a control parameter ϵ is varied. The solid lines represent a branch of front solutions with speed c . (b) Unfolding the bifurcation near the critical point ϵ_c gives an S-shaped relation in the unfolding parameter P .

*Electronic address: aric@lanl.gov

†Electronic address: ehud@bgumail.bgu.ac.il

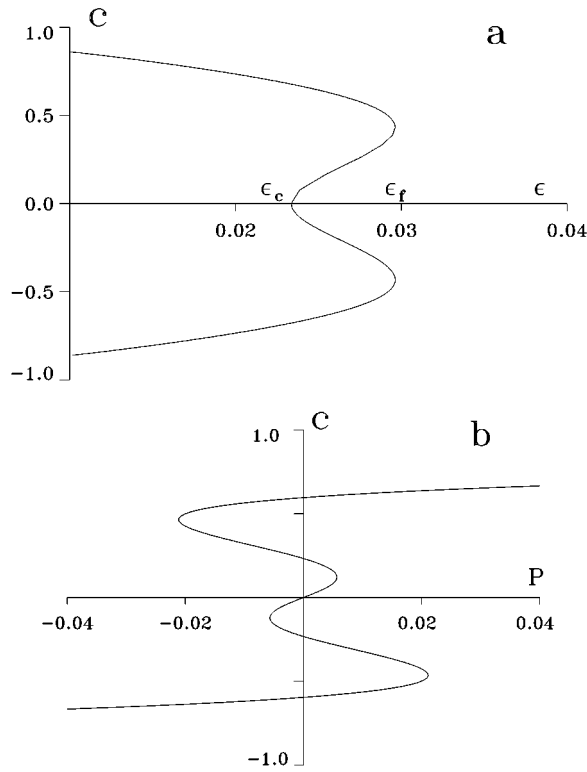


FIG. 2. Bifurcation diagrams for pulse solutions in the excitable FHN system. (a) A typical relation for the pulse speed c vs the system parameter ϵ gives a subcritical pitchfork bifurcation. (b) Unfolding the bifurcation near the critical point ϵ_c gives a multiple S-shaped curve for c in the unfolding parameter P .

critical value of the bifurcation parameter ϵ_f , at which the upper and lower branches in Fig. 2(a) terminate, designates the failure of propagation. Reversals in the direction of propagation (rather than collapse) have been observed in experiments on the Belousov-Zhabotinsky reaction subjected to an electric field [14].

In two space dimensions a local collapse of a spatially extended pulse amounts to a wave breakup. By numerically integrating a FitzHugh-Nagumo (FHN)-type model, we demonstrate two scenarios of wave breakups: breakup induced by an advective field, modeling an electric field in the BZ reaction, and breakup induced by a transverse (or lateral) instability. The two scenarios, observed in both experiments [1,2] and numerical simulations [1,9], reflect the *same* mechanism: the ability of weak perturbations to drive transitions from one of the pulse branches to the uniform attractor when the system is close to failure of propagation.

In Sec. II we describe the derivation of a pulse bifurcation diagram for a FHN model. The derivation applies to both excitable and bistable media. The information contained in this diagram is used to draw the propagation failure line in an appropriate parameter space. In Sec. III we consider the unfolding of the pulse bifurcation by an advective field and demonstrate wave breakup near the propagation failure. The unfolding by curvature is studied in Sec. IV and wave breakup induced by a transverse instability is demonstrated. We conclude in Sec. V with a discussion.

II. A BIFURCATION DIAGRAM FOR PULSE SOLUTIONS

We derive the pulse bifurcation diagram using an activator-inhibitor model of the FHN type. We assume that the activator varies on a time scale much shorter than that of the inhibitor and use singular perturbation theory [15–17]. Specifically, we study the pair of equations

$$u_t = \epsilon^{-1}(u - u^3 - v) + \delta^{-1}\nabla^2 u, \quad (1)$$

$$v_t = u - a_1 v - a_0 + \nabla^2 v,$$

where $\mu = \epsilon/\delta \ll 1$ and the subscripts t denote partial derivatives with respect to time. We consider a periodic wave train of planar (uniform along one dimension) pulses traveling at constant speed c in the x direction. Each of the excited (or “up-state”) domains occupies a length of λ_+ . The recovery (or “down-state”) domains are of length λ_- . In regions where u varies on a scale of order unity Eqs. (1) reduce to

$$\begin{aligned} v_{\chi\chi} + cv_{\chi} + u_+(v) - a_1 v - a_0 &= 0, & -\lambda_- < \chi < 0 \\ v_{\chi\chi} + cv_{\chi} + u_-(v) - a_1 v - a_0 &= 0, & 0 < \chi < \lambda_+, \end{aligned} \quad (2)$$

where $\chi = x - ct$ and $u_{\pm}(v)$ are the outer solution branches of the cubic equation $u - u^3 - v = 0$. For a_1 sufficiently large we may linearize the branches $u_{\pm}(v)$ around $v = 0$,

$$u_{\pm}(v) \approx \pm 1 - v/2. \quad (3)$$

We solve Eqs. (2) using the boundary conditions

$$v(-\lambda_-) = v_b, \quad (4)$$

$$v(0) = v_f,$$

$$v(\lambda_+) = v_b,$$

where v_f and v_b are yet undetermined, and the linear approximation (3). The solutions are

$$v = A_+ \exp(\sigma_1 \chi) + B_+ \exp(\sigma_2 \chi) + v_+, \quad -\lambda_- < \chi < 0$$

$$v = A_- \exp(\sigma_1 \chi) + B_- \exp(\sigma_2 \chi) + v_-, \quad 0 < \chi < \lambda_+,$$

with

$$\sigma_{1,2} = -\frac{c}{2} \pm \sqrt{\frac{c^2}{4} + a_1 + 1/2},$$

$$A_{\pm} = \frac{(v_b - v_{\pm}) - (v_f - v_{\pm}) \exp(\mp \sigma_2 \lambda_{\mp})}{\exp(\mp \sigma_1 \lambda_{\mp}) - \exp(\mp \sigma_2 \lambda_{\mp})},$$

$$B_{\pm} = \frac{-(v_b - v_{\pm}) + (v_f - v_{\pm}) \exp(\mp \sigma_1 \lambda_{\mp})}{\exp(\mp \sigma_1 \lambda_{\mp}) - \exp(\mp \sigma_2 \lambda_{\mp})},$$

and $v_{\pm} = (\pm 1 - a_0)/(a_1 + 1/2)$. Matching the derivatives of the solutions at $\chi = 0$, $v'(0^-) = v'(0^+)$, and imposing periodicity on the derivatives $v'(-\lambda_-) = v'(\lambda_+)$, we obtain two conditions

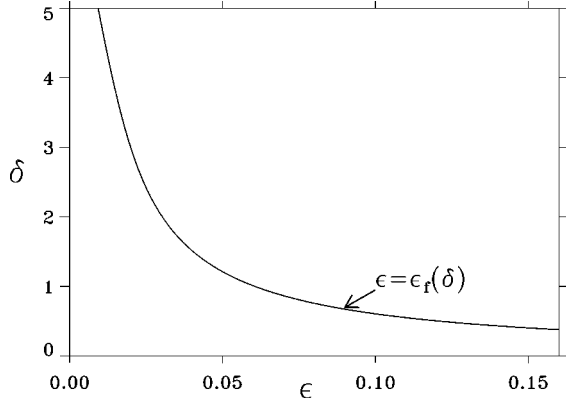


FIG. 3. Pulse failure propagation boundary in the ϵ - δ parameter plane for the excitable FHN model. To the right of the line pulses fail to propagate. The parameters are $a_1=1.25$ and $a_0=-0.2$.

$$\sigma_1 A_+ + \sigma_2 B_+ = \sigma_1 A_- + \sigma_2 B_-, \quad (5a)$$

$$\begin{aligned} \sigma_1 A_+ \exp(-\sigma_1 \lambda_-) + \sigma_2 B_+ \exp(-\sigma_2 \lambda_-) \\ = \sigma_1 A_- \exp(\sigma_1 \lambda_+) + \sigma_2 B_- \exp(\sigma_2 \lambda_+). \end{aligned} \quad (5b)$$

Two more conditions are obtained by studying the ‘‘front’’ and the ‘‘back,’’ that is, the leading and trailing border regions between the excited and recovery domains. Stretching the spatial coordinate according to $\zeta = \chi/\sqrt{\mu}$ gives the non-linear eigenvalue problems

$$u_{\zeta\zeta} + c \eta u_{\zeta} + u - u^3 - v_f = 0, \quad (6)$$

$$u(\zeta) \rightarrow u_-(v_f) \text{ as } \zeta \rightarrow \infty,$$

$$u(\zeta) \rightarrow u_+(v_f) \text{ as } \zeta \rightarrow -\infty,$$

for the narrow front region and

$$u_{\zeta\zeta} + c \eta u_{\zeta} + u - u^3 - v_b = 0, \quad (7)$$

$$u(\zeta) \rightarrow u_+(v_b) \text{ as } \zeta \rightarrow \infty,$$

$$u(\zeta) \rightarrow u_-(v_b) \text{ as } \zeta \rightarrow -\infty,$$

for the narrow back region. Here $\eta = \sqrt{\epsilon\delta}$. Solutions of Eqs. (6) and (7) yield

$$c \eta = -\frac{3}{\sqrt{2}} v_f, \quad (8)$$

$$c \eta = \frac{3}{\sqrt{2}} v_b, \quad (9)$$

respectively.

Substituting relations (8) and (9) into Eqs. (5) leaves two equations for the three unknowns λ_+ , λ_- , and c . The one-parameter family of solutions describes periodic wave trains of pulses traveling with speed

$$c = \mathcal{C}(\lambda; \eta, a_0, a_1), \quad (10)$$

where $\lambda = \lambda_+ + \lambda_-$ is the varying wavelength of the family. The graph of c versus λ provides the dispersion relation

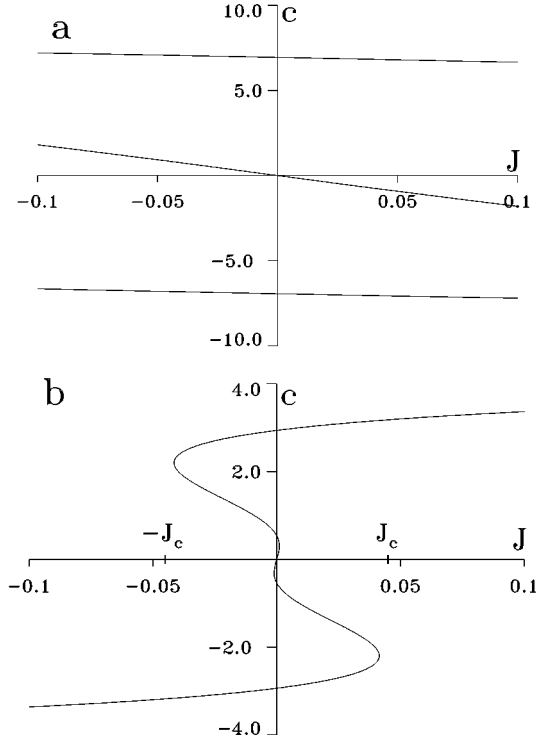


FIG. 4. Solutions of the speed c vs advection J relation (12). (a) Away from the bifurcation point, variations in J have little effect on the pulse speed ($\epsilon=0.01$). (b) Near the bifurcation point, small variations in J may drive the system past the end point of the solution branch and cause pulse collapse ($\epsilon=0.05$). Other parameters are $a_1=1.25$, $a_0=-0.2$, and $\delta=1.0$.

curve obtained in earlier studies [15,16]. Our interest here is with the behavior of a single pulse and therefore only the limit of large λ will be considered. We remind the reader that in deriving these equations we have assumed $\mu = \epsilon/\delta \ll 1$, which excludes very small δ values.

We solved Eqs. (5) numerically for both excitable and bistable systems at large values of the period λ . The solutions were computed by numerical continuation of known solutions when $a_0=0$ and $\lambda_+ = \lambda_-$. They yield the typical bifurcation diagram for the speed c in terms of the parameter ϵ as shown in Fig. 2(a). At some critical value ϵ_f , the branch of solutions terminates and past that point pulses fail to propagate. The value of ϵ_f depends on the other system parameters as well. Figure 3 shows a graph of $\epsilon = \epsilon_f(\delta)$ for an excitable system.

Note the inherent subcritical nature of the bifurcation [18,19]. The bifurcation becomes supercritical only in the limit $a_0 \rightarrow 0$ (pertaining to a bistable medium) where the pulse size tends to infinity. In that limit Eqs. (5) can easily be solved. The solutions are $c=0$ and $c = \pm (2q/\eta) \sqrt{\eta_c^2 - \eta^2}$ for $\eta < \eta_c$ and coincide with the nonequilibrium Ising-Bloch bifurcation for front solutions [20].

III. WAVE BREAKUP BY AN ADVECTIVE FIELD

Application of an electric field to a chemical reaction involving molecular and ionic species, like the BZ reaction, results in a differential advection [21]. Differential advection in the FHN equations can be modeled (without loss of gen-

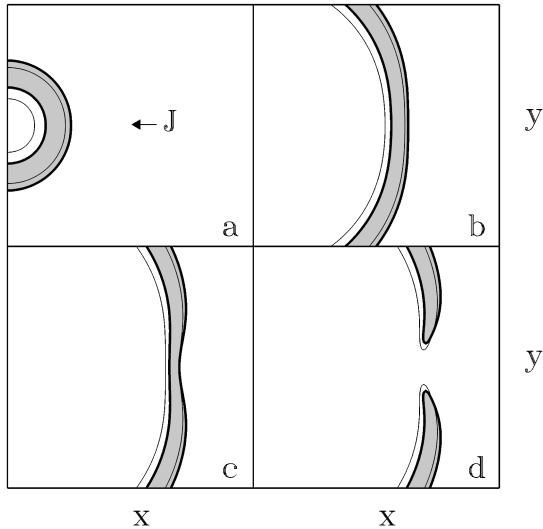


FIG. 5. Numerical solution of Eqs. (11) with a weak advective field $\mathbf{J} = J\hat{\mathbf{x}}$. The thick and thin lines pertain to $u=0$ and $v=0$ contour lines, respectively. The initial circular pulse fails to propagate along the direction of the advective field and the pulse breaks. The pulse continues to propagate in directions different from the advective field. The equation parameters are the same as in Fig. 4.

erality) by adding an advective term to the inhibitor equation

$$u_t = \epsilon^{-1}(u - u^3 - v) + \delta^{-1}\nabla^2 u, \quad (11)$$

$$v_t = u - a_1 v - a_0 + \mathbf{J} \cdot \nabla v + \nabla^2 v,$$

where \mathbf{J} is a constant vector. Looking for planar solutions propagating at constant speeds in the \mathbf{J} direction and rescaling ϵ and δ by the factor $c/(c+J)$ we find the influence on the pulse speed by the advection

$$c + J = \mathcal{C} \left(\lambda; \frac{c}{c+J} \eta, a_0, a_1 \right), \quad (12)$$

where \mathcal{C} is defined in Eq. (10). Figure 4 shows the dependence of the pulse speed c on the advection constant J obtained by numerically solving Eq. (12) for large λ . Away from failure of propagation (ϵ is significantly smaller than ϵ_f) small variations of J have little effect on the pulse motion [Fig. 4(a)]. However, close to failure, such variations can induce wave breakup by driving the system past the endpoint $J = J_c$ [Fig. 4(b)].

Figure 5 shows a numerical simulation of Eqs. (11) with $\mathbf{J} = J\hat{\mathbf{x}}$ and an initial condition of a curved pulse. Along the pulse the effective advection field is the projection of \mathbf{J} onto the direction of propagation at that point. With $J=0$ the curved pulse propagates uniformly outward in a circular ring. Choosing J slightly greater than J_c , a wave breakup results: The part of the pulse propagating in the $\hat{\mathbf{x}}$ direction fails to propagate. Those parts propagating in significantly different directions still propagate. These results explain earlier observations of wave breakup induced by electric fields [1].

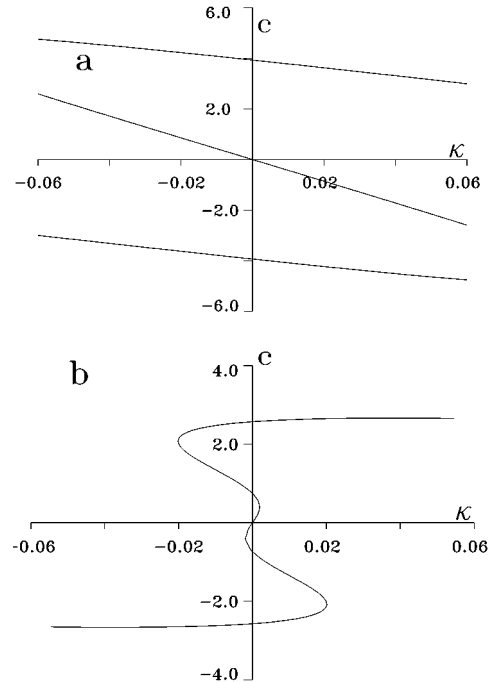


FIG. 6. Solutions to the speed vs curvature relation (14). (a) Away from the bifurcation point (top), the speed c varies approximately linearly with the curvature κ ($\epsilon = 0.003$). (b) Near the bifurcation point, small curvature variations may drive the system past the end point of the solution branch and cause pulse collapse ($\epsilon = 0.022$). Other parameters are $a_1 = 1.25$, $a_0 = -0.2$, and $\delta = 2.5$.

IV. WAVE BREAKUP INDUCED BY A TRANSVERSE INSTABILITY

Spatially extended pulses, such as stripes or disks, may be unstable to transverse perturbations along the pulse line. Ohta, Mimura, and Kobayashi studied the case of deforma-

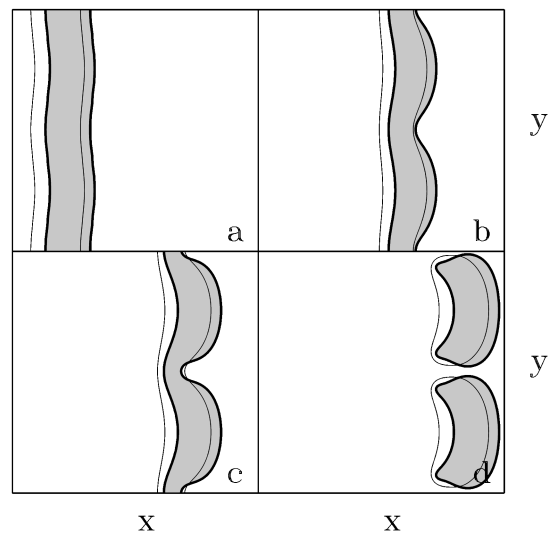


FIG. 7. Breakup of a pulse by transverse instability. The thick and thin lines pertain to $u=0$ and $v=0$ contour lines, respectively. The initial almost planar pulse is unstable to transverse perturbations and forms a dent. The dent grows and the pulse breaks at the region of high curvature. The equation parameters are the same as in Fig. 6.

tions of planar and disk-shaped stationary patterns in a piecewise linear FitzHugh-Nagumo model [22]. Kessler and Levine derived conditions for the transverse instability of traveling stripes in a piecewise linear version of the Oregonator [23]. The curvature induced by a transverse instability can lead to the formation of labyrinthine patterns [8,24,25] or cause spontaneous breakup of a pulse as we will now show.

For the model of Eqs. (1), the effect of curvature κ on pulse propagation can be obtained from Eq. (10) by rewriting the equations in a frame moving with the pulse [26]. Assuming that the radius of curvature is much larger than the pulse width and assuming a negligible dependence of u and v on arclength and time (in the moving frame) we obtain

$$\begin{aligned} \delta^{-1}u'' + (c + \delta^{-1}\kappa)u' + \epsilon^{-1}(u - u^3 - v) &= 0, \\ v'' + (c + \kappa)v' + u - a_1v - a_0 &= 0, \end{aligned} \quad (13)$$

where the prime denotes differentiation with respect to a coordinate normal to the front line. Rescaling ϵ and δ by the factor $(c + \delta^{-1}\kappa)/(c + \kappa)$ Eq. (10) becomes

$$c + \kappa = \mathcal{C}\left(\lambda; \frac{c + \delta^{-1}\kappa}{c + \kappa} \eta, a_0, a_1\right). \quad (14)$$

Figure 6 shows numerical solutions of Eq. (14) for c in terms of κ . Far away from the failure of propagation [Fig. 6(a)] we find the usual approximate linear c - κ relations for right ($c > 0$) and left ($c < 0$) propagating pulses [15,17]. Close to failure [Fig. 6(b)], small realizable curvature variations may cause collapse.

Equation (14) contains information also about the transverse stability of a pulse line. A positive slope of a c - κ relation at $\kappa=0$ indicates an instability of a planar pulse. Figure 7 shows a simulation of Eqs. (1) at parameter values pertaining to the c - κ relation in Fig. 6(b). Starting with a near planar pulse, dents grow due to a transverse instability. The negative curvature that develops induces a wave breakup.

V. CONCLUSION

We have identified a mechanism for breakup of waves in an excitable media. The key ingredient of this mechanism is the proximity to a subcritical pitchfork pulse bifurcation [as shown in Fig. 2(a)]. Near the bifurcation small perturbations become significant and may induce the failure of propagation. The nature of the perturbation is of secondary importance. As illustrated in Figs. 4(b) and 6(b), the effects of an advective field and curvature are similar; they both induce wave breakup by driving the system past the end points of propagating pulse branches. A perturbation inducing breakup can be externally applied, such as an electric field in the BZ reaction, or spontaneously formed, such as curvature growth by a transverse instability. An interesting question not resolved in this study is the observed preference of propagation failure or collapse rather than reversal in the direction of propagation.

ACKNOWLEDGMENTS

This study was supported in part by Grant No. 95-00112 from the U.S.-Israel Binational Science Foundation.

-
- [1] J. J. Taboada *et al.*, *Chaos* **4**, 519 (1994).
 - [2] M. Markus, G. Kloss, and I. Kusch, *Nature (London)* **371**, 402 (1994).
 - [3] M. Courtemanche and A. T. Winfree, *Int. J. Bifurcation Chaos* **1**, 431 (1991).
 - [4] A. V. Holden and A. V. Panfilov, *Int. J. Bifurcation Chaos* **1**, 219 (1991).
 - [5] A. Karma, *Phys. Rev. Lett.* **71**, 1103 (1993).
 - [6] M. Bär and M. Eiswirth, *Phys. Rev. E* **48**, R1635 (1993).
 - [7] M. Bär *et al.*, *Chaos* **4**, 499 (1994).
 - [8] A. Hagberg and E. Meron, *Phys. Rev. Lett.* **72**, 2494 (1994).
 - [9] A. F. M. Maree and A. V. Panfilov, *Phys. Rev. Lett.* **78**, 1819 (1997).
 - [10] C. Elphick, A. Hagberg, and E. Meron, *Phys. Rev. E* **51**, 3052 (1995).
 - [11] A. Hagberg and E. Meron, *Nonlinear Science Today* (1996), (<http://www.springer-ny.com/nst/>) PII:S09389008(96)00013-7.
 - [12] P. Couillet, J. Lega, B. Houchmanzadeh, and J. Lajzerowicz, *Phys. Rev. Lett.* **65**, 1352 (1990).
 - [13] A. Hagberg and E. Meron, *Nonlinearity* **7**, 805 (1994).
 - [14] H. Sevcikova, M. Marek, and S. C. Muller, *Science* **257**, 951 (1992).
 - [15] J. J. Tyson and J. P. Keener, *Physica D* **32**, 327 (1988).
 - [16] J. D. Dockery and J. P. Keener, *SIAM (Soc. Ind. Appl. Math.) J. Appl. Math.* **49**, 539 (1989).
 - [17] E. Meron, *Phys. Rep.* **218**, 1 (1992).
 - [18] P. Schütz, M. Bode, and V. V. Gafiichuk, *Phys. Rev. E* **52**, 4465 (1995).
 - [19] E. M. Kuznetsova and V. V. Osipov, *Phys. Rev. E* **51**, 148 (1995).
 - [20] A. Hagberg and E. Meron, *Chaos* **4**, 477 (1994).
 - [21] S. P. Dawson, A. Lawniczak, and R. Kapral, *J. Chem. Phys.* **100**, 5211 (1994).
 - [22] T. Ohta, M. Mimura, and R. Kobayashi, *Phys. Rev. D* **34**, 115 (1989).
 - [23] D. A. Kessler and H. Levine, *Phys. Rev. A* **41**, 5418 (1990).
 - [24] R. E. Goldstein, D. J. Muraki, and D. M. Petrich, *Phys. Rev. E* **53**, 3933 (1996).
 - [25] C. B. Muratov and V. V. Osipov, *Phys. Rev. E* **53**, 3101 (1996).
 - [26] A. Hagberg and E. Meron, *Phys. Rev. Lett.* **78**, 1166 (1997).